

Star Formation in a Turbulent Framework: From Giant Molecular Clouds to Protostars

Dávid Guszejnov^{1*} and Philip F. Hopkins¹

¹ *TAPIR, Mailcode 350-17, California Institute of Technology, Pasadena, CA 91125, USA*

Submitted to MNRAS, 27 July 2015

ABSTRACT

Turbulence is thought to be a primary driving force behind the early stages of star formation. In this framework large, self gravitating, turbulent clouds fragment into smaller clouds which in turn fragment into even smaller ones. At the end of this cascade we find the clouds which collapse into protostars. Following this process is extremely challenging numerically due to the large dynamical range so in this paper we propose a semi analytic framework which is able to follow this process from the largest, giant molecular cloud (GMC) scale, to the final protostellar size scale. Due to the simplicity of the framework it is ideal for theoretical experimentation to find the principal processes behind different aspects of the star formation process. The basic version of the model discussed in this paper only contains turbulence, gravity and very crude assumptions about feedback, nevertheless it can reproduce the observed core mass function (CMF) and provide the protostellar system mass function (PSMF), which shows a striking resemblance to the observed IMF which implies that other physics do not change the IMF qualitatively. Furthermore we find that to produce a universal IMF protostellar feedback must be taken into account otherwise the PSMF peak shows a strong dependence on the background temperature.

Key words: stars: formation – turbulence – galaxies: evolution – galaxies: star formation – cosmology: theory

1 INTRODUCTION

Finding a comprehensive description of star formation has been one of the principal challenges of astrophysics for decades. Such a model would prove invaluable to understanding the evolution of galactic structures, binary star systems and even the formation of planets.

It has been long established that stars form from collapsed dense molecular clouds (McKee & Ostriker 2007). Currently the most promising candidate for a driving process is turbulence, as it can create subregions with sufficiently high density so that they become self gravitating on their own, while also exhibiting close to scale free behavior (in accordance with the observations of Larson 1981; Bolatto et al. 2008). These fragments are inherently denser than their parents so they collapse faster, quasi independent from their surroundings. However, once they turn into stars they start heating up the surrounding gas (by radiation, solar winds or supernova explosions) preventing it from collapsing and forming stars (see Fig. 1). This process is inherently hierarchical so it should be possible to derive a model that follows it from the scale of the largest self gravitating clouds, the GMCs (100 pc), to the scale of protostars (10^{-5} pc). This is

not possible in direct hydrodynamic simulations due to resolution limits, but can be treated approximately in analytic and semi-analytic models.

This paradigm has been explored by Padoan et al. (1997) and Padoan & Nordlund (2002), then made more rigorous by Hennebelle & Chabrier (2008) who attempted to create an analytic model analogous to Press & Schechter (1974), which approximates the background density field as a Gaussian random field. Later Hopkins (2012a) expanded on these works by adopting the excursion set formalism to find the distribution of the largest self gravitating structures, which was found to be very similar to the observed distribution of GMCs. Similarly Hopkins (2012b) found that the distribution of the smallest self gravitating structures fit well the observed CMF. Building on these results Hopkins (2013a) generalized the formalism to be applicable to systems with different equations of state and turbulent properties. Utilizing these results Guszejnov & Hopkins (2015) incorporated the time dependent collapse of the cores to find the distribution of protostars which closely reproduced the observed IMF.

These models did successfully reproduce the CMF, IMF and the GMC mass function, however they had several shortcomings. First, they did not account for the differences in formation and collapse times of clouds of different sizes (e.g. small clouds form faster and collapse faster). Secondly, the

* E-mail: guszejnov@caltech.edu

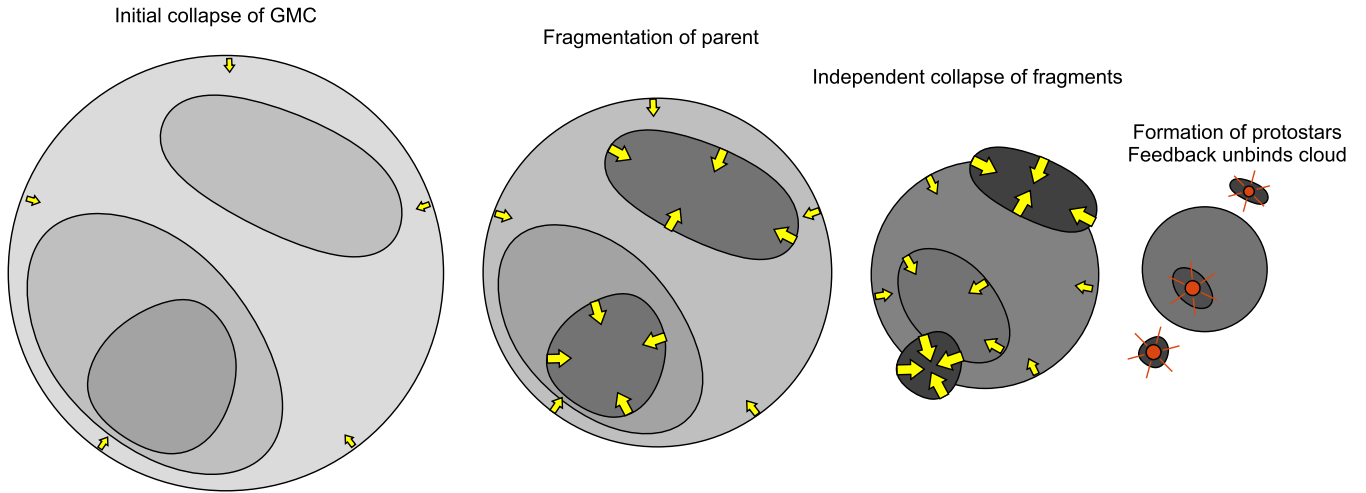


Figure 1. Evolution of collapsing clouds, with time increasing from left to right (darker subregions are higher-density, arrows denote regions which are independently self-gravitating and become thicker with increasing collapse rate). As the initial cloud collapses, density fluctuations increase (because gravitational energy pumps turbulence), creating self-gravitating subregions. These then collapse independently from the parent cloud, forming protostars at the end. These protostars can provide a sufficiently strong feedback that the rest of the cloud becomes unbound and ceases to collapse.

excursion set formalism describes the density field around a random Lagrangian point. This means that the spatial structure of a cloud can not be modeled directly (e.g. there is no way to find if a cloud forms binary stars). Finally, there is no self consistent excursion set model that follows from the GMC to the protostar scale (i.e. [Hopkins 2012b](#) covered scales between the galactic disk and cores, [Guszejnov & Hopkins 2015](#) between cores and protostars). We believe these shortcomings can be overcome by moving away from the analytic excursion set formalism and instead adopting a simple semi-analytical approach with the same random field assumption. This framework would allow us to follow the evolution self gravitating clouds while resolving both the GMC and protostellar scales and preserving spatial information. In this paper we will outline a possible candidate for such a model.

The paper is organized as follows. Sec. 2 provides a general overview of the model, including the primary assumptions and approximations and briefly outlines its numerical realization. Sec. 3 shows the simulated time evolution of the CMF and the protostellar system mass function (PSMF) which shows a striking similarity to the IMF. Sec. 3.2 also discusses the effects of having a temperature independent equation of state on the peak of the PSMF and the universality of the IMF. Finally, Sec. 4 discusses the results and further applicability of the model.

2 METHODOLOGY

In short, instead of doing a detailed hydrodynamical simulation involving gravity and radiation, our model assumes a simple stationary model for the density field, collapse of structures at constant virial parameter and an equation of state that depends on cloud properties. Starting from a GMC sized cloud it evolves the density field as the cloud collapses and pumps turbulence. At each step, we search for self gravitating structures which we treat as new frag-

ments, for which the process is repeated in recursion until a substructure is found that collapses to protostellar scale without fragmenting. This process and our assumptions will be discussed in more detail in the following subsections.

Our model is a modified version of the excursion set model used by [Guszejnov & Hopkins \(2015\)](#) (henceforth referred to as Paper I) using the theoretical foundation of [Hopkins \(2013a\)](#) (henceforth referred to as Paper II). Due to the significant overlap between models we show only the essential equations and emphasize the differences and their consequences. If the reader is familiar with Paper I we suggest skipping to Sec. 2.3.

2.1 The Density Field

It is known that the density field in the cases of both sub and supersonic, isothermal flows follows approximately lognormal statistics (for corrections see [Hopkins \(2013b\)](#)). This means that if we introduce the density contrast $\delta(\mathbf{x}) = \ln[\rho(\mathbf{x})/\rho_0] + S/2$, with $\rho(\mathbf{x})$ as the local density, ρ_0 as the mean density and S as the variance of $\ln \rho$, it would follow a close to Gaussian distribution¹, thus

$$P(\delta|S) \approx \frac{1}{2\pi S} \exp\left(-\frac{\delta^2}{2S}\right). \quad (1)$$

¹ It is a common misconception that analytical models such as the one presented in this paper take the total density distribution to be purely lognormal. While the density distribution in each cloud/fragment is indeed assumed to be locally lognormal on a single timestep, these have different means and deviations (see Eq. 2) depending on their initial conditions and time, which means that the total distribution will be different. If we measure the density distribution in our calculations (see Fig. 2), we find it is approximately lognormal at low densities (set by the lowest density structure: the parent cloud), while the high mass end becomes a power law as it is a mass weighted average of the distributions for different substructures whose mass distribution is a power law (see Fig. 4).

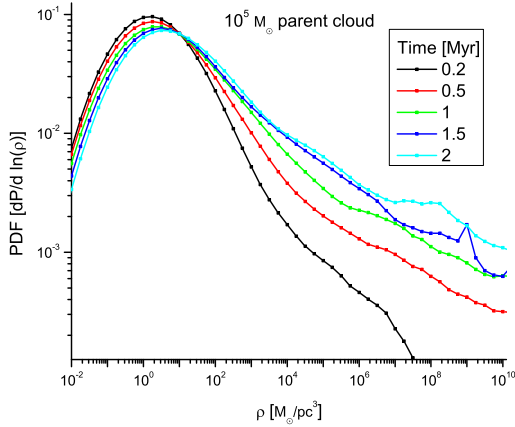


Figure 2. Time evolution of the distribution of density in a parent GMC of $10^5 M_{\odot}$. This is a mass weighted average of the density distribution of all substructures in the parent cloud (which are all assumed to be lognormal with different parameters), thus the low mass end is set by the lowest density structure which is the parent cloud while the high mass end is a power law due to the power law like distribution of fragments (see Fig. 4).

It is a property of normal and lognormal random variables that a linear functional of these variables will also be normal/lognormal, thus the averaged density in a region has lognormal equilibrium statistics whose properties are prescribed by turbulence. Following Paper II this yields

$$S(\lambda) = \int_0^{\lambda} \Delta S(\lambda) d \ln \lambda \approx \int_0^{\lambda} \ln [1 + b^2 \mathcal{M}^2(\lambda)] d \ln \lambda, \quad (2)$$

where λ is the averaging scale, $\mathcal{M}(\lambda)$ is the Mach number of the turbulent velocity dispersion on scale λ and b is the fraction of the turbulent kinetic energy in compressive motions, which we take to be about $1/2$ (this is appropriate for an equilibrium mix of driving modes, see Federrath et al. 2008 for details. Paper I experimented with $b \sim 1/4 - 1$ and found no qualitative differences).

It is important to note that although ρ is lognormal which means δ is Gaussian, there is significant spatial correlation (i.e. ρ can not change instantly over arbitrarily small spatial intervals) so it is not possible to model the density field as a spatially independent random field. To circumvent this issue we solve the problem in Fourier space since $\delta(k)$ is also lognormal, while there is little correlation between modes so it is acceptable to assume them to be independent (note: having correlated modes in Fourier space introduces only mild effects on the final mass functions, see Appendix A of Paper II for details). Combined with the fact that the number of modes in the $[k, k + dk]$ range is $dN(k) = (4\pi k^2 dk) n_k$, where n_k is the mode density, we get the variance for an individual density contrast mode is

$$S_{\text{mode}}(\mathbf{k}) = \frac{\ln(1 + b^2 \mathcal{M}(k)^2)}{4\pi k^3 n_k}. \quad (3)$$

Paper II showed that to realize a steady state density contrast field with such variance and zero mean, the Fourier

component $\delta(\mathbf{k}, t)$ must evolve as

$$\delta(\mathbf{k}, t + \Delta t) = \delta(\mathbf{k}, t) (1 - \Delta t / \tau_k) + \mathcal{R} \sqrt{2S_{\text{mode}}(\mathbf{k}) \Delta t / \tau_k}, \quad (4)$$

where \mathcal{R} is a Gaussian random number with zero mean and unit variance while $\tau_k \sim v_t(k) / \lambda$ is the turbulent crossing time on scale $\lambda \sim 1/k$, and the turbulence dispersion obeys $v_t^2(\lambda) \propto \lambda^{p-1}$ thus $\tau_k \propto \lambda^{\frac{p-3}{2}}$ (in our simulations we use $p = 2$, appropriate for supersonic turbulence, see (Murray 1973; Schmidt et al. 2009)).

2.1.1 The Equation of State

It is easy to convince oneself that a purely isothermal or polytropic equation of state (EOS) would be a very poor description of the complex physical processes contributing to the cooling and heating of clouds, however, modeling these processes in detail would require full numerical simulations. Instead we try to find a simple, heuristic EOS that captures the behaviors critical to our calculation. One of the most important effect during collapse is the transitioning from the state where the cooling radiation efficiently escapes from the cloud to the state where the cloud becomes optically thick to it and heats up as it contracts. We adopt the same effective polytropic EOS model as Paper I where for small time steps (compared to the dynamical time):

$$T(\mathbf{x}, t + \Delta t) = T(\mathbf{x}, t) \left(\frac{\rho(\mathbf{x}, t + \Delta t)}{\rho(\mathbf{x}, t)} \right)^{\gamma(\Sigma) - 1}. \quad (5)$$

where $\Sigma = M / (4\pi R^2)$ is the surface density of the cloud and $\gamma(\Sigma)$ is the effective polytropic index which depends on the global surface density of the cloud with the following relation:

$$\gamma(\Sigma) = \begin{cases} 0.7 & \Sigma < 3 M_{\odot} / \text{pc}^2 \\ 0.094 \ln \left(\frac{\Sigma}{3 M_{\odot} / \text{pc}^2} \right) + 0.7 & 3 < \frac{\Sigma}{M_{\odot} / \text{pc}^2} < 5000 \\ 1.4 & \Sigma > 5000 M_{\odot} / \text{pc}^2 \end{cases}. \quad (6)$$

This $\gamma(\Sigma)$ equation of state does capture the physics of the limit where the cloud is optically thick to its own cooling radiation, however in the optically thin limit the local density ρ determines the effective polytropic index, not Σ . Nevertheless this EOS is still useful as the optically thin limit is populated by massive clouds whose fragmentation is barely dependent on the value of γ (see Paper I) so changing to a ρ dependent EOS for less dense clouds would not make a significant difference.

2.2 Collapse: criterion and evolution

It has been shown in Paper I and Paper II that the critical density for a (compared to the galactic disk) small, homogeneous, spherical region of radius R to become self gravitating is

$$\frac{\rho_{\text{crit}}(R)}{\rho_0} = \frac{1}{1 + \mathcal{M}_{\text{edge}}^2} \left(\frac{R}{R_0} \right)^{-2} \left[\left(\frac{T(R)}{T_0} \right) + \mathcal{M}_{\text{edge}}^2 \left(\frac{R}{R_0} \right)^{p-1} \right], \quad (7)$$

where the two terms represent thermal and turbulent energy respectively. $T(\lambda)$ is the temperature averaged over the

scale λ , while T_0 is the mean temperature of the whole collapsing cloud and we used the following scaling of the turbulent velocity dispersion and Mach number \mathcal{M}

$$\mathcal{M}^2(R) \equiv \frac{v_t^2(R)}{\langle c_s^2(\rho_0) \rangle} = \mathcal{M}_{\text{edge}}^2 \left(\frac{R}{R_0} \right)^{p-1}, \quad (8)$$

where R_0 is the size of the self gravitating parent cloud and p is the turbulent spectra index, so the turbulent kinetic energy scales as $E(R) \propto R^p$; generally $p \in [5/3; 2]$, but in this paper, just like in Paper I we assume $p = 2$ as is appropriate for supersonic turbulence.

Our goal is to create a model that resolves clouds from GMC to protostellar scales, so the initial structures of the model are the GMCs which themselves are self gravitating (first crossing scale in the excursion set formalism). This means they must satisfy Eq. 7, which for spherical clouds ($M(R) = (4\pi/3) R^3 \rho(R)$) in isothermal parents yields the mass-size relation:

$$M = \frac{M_{\text{sonic}}}{2} \frac{R}{R_{\text{sonic}}} \left(1 + \frac{R}{R_{\text{sonic}}} \right). \quad (9)$$

Note that for very high mass clouds a correction containing the angular frequency of the galactic disk would appear, however this term is small (see Paper II for details). Eq. 9 introduces R_{sonic} which is the sonic length, the scale on which the turbulent velocity dispersion is equal to the sound speed, so in an isothermal cloud using the scaling of Eq. 8, we expect

$$R_{\text{sonic}} = R_0 \mathcal{M}_{\text{edge}}^{-2/(p-1)}. \quad (10)$$

Meanwhile M_{sonic} is defined as the minimum mass required for a sphere with R_{sonic} radius to start collapsing so

$$M_{\text{sonic}} = \frac{2}{Q_{\text{coll}}} \frac{c_s^2 R_{\text{sonic}}}{G}, \quad (11)$$

where G is the gravitational constant and Q_{coll} is the virial parameter for a sphere of the critical mass for collapse (see Eq. 14 later). For reasonable galactic parameters and temperatures $R_{\text{sonic}} \approx 0.1$ pc and $M_{\text{sonic}} \approx 6.5 M_{\odot}$ (assuming we use the value for Q_{coll} we specify in Sec. 2.2.1).

Since the GMC in question has just started collapsing, the turbulent velocity at its edge must (initially) obey the turbulent power spectrum. Thus $v_t^2(R) \propto R$ for the supersonic and $v_t^2(R) \propto R^{2/3}$ (the Kolmogorov scaling) for the subsonic case. Using the mass-size relation of Eq. 9 leads to the following fitting function

$$\frac{(1 + \mathcal{M}_{\text{edge}}^2) \mathcal{M}_{\text{edge}}^2}{1 + \mathcal{M}_{\text{edge}}^{-1}} = \frac{M}{M_{\text{sonic}}}, \quad (12)$$

which exhibits scalings of $M \propto \mathcal{M}^3$ for the subsonic and $M \propto \mathcal{M}^4$ for the supersonic case respectively, and (coupled to the size-mass relation above) very closely reproduces the observed linewidth-size relations (Larson 1981; Bolatto et al. 2008; Lada & Lada 2003). Note that dense regions will deviate from this scaling, as observed (see references above), because collapse 'pumps' energy into turbulence.

2.2.1 Evolution of Collapsing Clouds

One of the key assumptions of the previous models in Paper I and Paper II is that the kinetic energy of collapse pumps

turbulence whose energy is dissipated on a crossing time. As turbulent motion provides support against collapse, the collapse can only continue after this extra energy has been dissipated by turbulence (see Sec. 9.2 in Paper II for details). This leads to the following equation for the contraction of the cloud:

$$\frac{d\tilde{r}}{d\tilde{t}} = -\tilde{r}^{-1/2} \left(1 - \frac{1}{1 + \mathcal{M}_{\text{edge}}^2(\tilde{r})} \right)^{3/2}, \quad (13)$$

where $\tilde{r}(t) = R(t)/R_0$ is the relative size of the cloud at time t while $\tilde{t} \equiv t/t_0$ is time, normalized to the initial cloud dynamical time $t_0 \sim 2Q_{\text{coll}}^{-3/2} (GM_0/R_0^3)^{-1/2}$ (see Paper II for derivation). In this case the initial dynamical time (t_0) and the crossing time only differ by a freely-defined order unity constant, so in our simulations we consider them to be equal without loss of generality.

The other key assumption of the model is that collapse happens at constant virial parameter. We define Q_{coll} as

$$Q_{\text{coll}} \frac{GM}{R} = c_s^2 + v_t^2 = c_s^2 (1 + \mathcal{M}_{\text{edge}}^2). \quad (14)$$

Note that Q_{coll} is not the Toomre Q parameter, merely the ratio of kinetic energy to potential energy needed to destabilize the cloud, thus the higher Q_{coll} the more unstable clouds are to fragmentation. One can find Q_{coll} using the Jeans criterion:

$$0 \geq \omega^2 = (c_s^2 + v_t^2) k^2 - 4\pi G \rho, \quad (15)$$

which for the critical case ($\omega = 0$) leads to

$$Q_{\text{coll}} = \frac{3}{k^2 R^2}. \quad (16)$$

One would be tempted to substitute in $k = 2\pi/R$, but that would be incorrect, as we have a spherical overdensity with R radius to which the corresponding sinusoidal wavelength is not R . We therefore chose $k = \frac{\pi}{2R}$ which yields $Q_{\text{coll}} = 12/\pi^2 \approx 1.2$. Note that all formulas contain $c_s^2/Q_{\text{coll}} \propto T/Q_{\text{coll}}$ so an uncertainty in the virial parameter is degenerate with an uncertainty in the initial temperature.

Combined, the above equations completely describe the collapse of a spherical cloud, as the EOS (Eq. 5-6) sets the temperature and thus the sound speed. Using that, Eq. 14 provides the edge Mach number, which allows us using Eq. 13 to calculate the contraction speed.

2.3 Differences from previous models

So far we are following the same assumptions as Paper I and Paper II, however, instead of simulating a stochastic density field averaged on different scales around a random Lagrangian point (the basis of analytic excursion set models) we use a grid in space and time. This means that we directly evolve the $\delta(k)$ modes to simulate the density field. This allows us to preserve spatial information as we now have information about the relative positions and velocities of substructures.

Having a proper density field not only allows us to take basic geometrical effects into account (as substructures are still assumed to be spherical) but it allows a proper application of the self gravitation condition of Eq. 7. The excursion set formalism finds the smallest self gravitating structure a point is embedded in. The problem is that this "last crossing"

structure may have further self gravitating fragments which do not contain the aforementioned point. These substructures will form protostars of their own (see Fig. 1) leaving their parent cloud with less mass which in turn might not be self gravitating anymore. This is not addressed in excursion set models which instead simply assume 100% of the mass ending up in protostars of different sizes (which of course is not realistic), while the proposed grid model predicts only about 5% (see Sec.3.2).

It should be noted that like the model of Paper I, in this first study we include no explicit feedback mechanism. Instead the model utilizes a few crude approximations to account for the qualitative effects of feedback. First, it is assumed that the clouds that becomes unbound by fragmentation stop collapsing and "linger" for a few dynamical times (during which they may form new self gravitating fragments) before being heated up/blown up by the newly created protostars in such a fashion that they can no longer participate in star formation. Like in Paper I we neglected the effects of accretion and protostellar fragmentation when comparing to the IMF as the protostellar system mass function (from now on *PSMF*) is already a good enough qualitative fit so their effects must be modest (except for the very high and low mass ends where fragmentation could provide a high mass cut off while accretion could affect the turnover point). We would also like to note that it is possible to apply a crude implementation of supernova feedback by simply stopping the evolution after a few Myrs (when enough supernovae have exploded to unbind the GMC). Since the simulation provides a time dependent output, it can be done during post-processing. Of course, the point of our framework is that one could easily add models for feedback, and/or accretion if desired.

We would like to note that using hydrodynamical simulations would allow a much more realistic treatment of certain details of the problem, however the large dynamic range ($10^{-5} - 100$ pc) and the long range gravitational interactions make such attempts extremely computationally intensive, preventing one from getting substantial statistics. A further issue with direct hydrodynamical simulations is that they involve the full, detailed form of all physical interactions, making it harder to pinpoint the primary driving mechanisms behind certain phenomena.

In summary we propose a semi-analytical model which has negligible computational cost but still captures phenomena (e.g. spatial correlation, motion of objects, complicated time dependence) which are beyond the capabilities of the analytical excursion set formalism.

3 EVOLUTION OF THE IMF AND CMF IN GMCs

In this section we present an application of the model for simulating the collapse of an ensemble of GMCs (distributed following the first crossing mass function obtained by Hopkins 2012b, see Fig. 3). This includes simulating a number of GMCs of different masses where the initial conditions are set by Eq. 8 and Eq. 9. The clouds are assumed to start with fully formed turbulence (as GMCs form out of an already turbulent medium) which means that before simulating the collapse the density field is initialized to have the

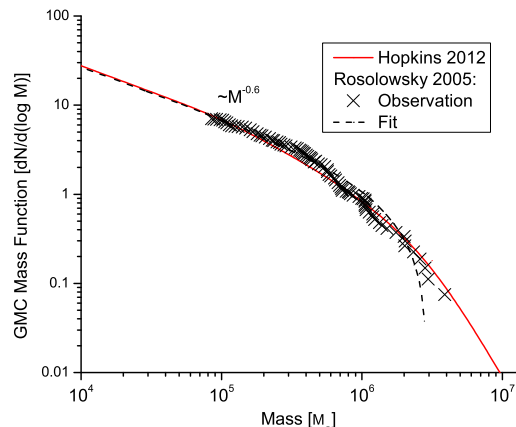


Figure 3. Initial mass function of GMCs according to the excursion set model of Hopkins (2012b) compared to the observations (X symbols) and empirical fitting function (dashed black line) of Rosolowsky (2005). The normalization of the plot is arbitrary.

appropriate lognormal distribution. The output of the code contains the formation time and properties (e.g. mass, position, velocity) of individual protostars along with snapshots of the hierarchical structure of bound objects at different times. In Sec. 3.1 we investigate the latter and compare the distribution of nonfragmented structures with the observed CMF. Later, in Sec. 3.2 we discuss the time evolution of PSMF and how it relates to the IMF and whether it can be universal without invoking feedback physics.

3.1 Fragmentation and self gravitating substructures

It is well known that during their collapse clouds fragment into smaller self gravitating structures (see Fig. 1). It is instructive to see how much mass is bound in structures of different sizes. Fig. 4 shows the time evolution of the number of structures of different sizes counting all "clouds in clouds", which follows a distribution similar to the observed IMF and CMF (for quick overview see Offner et al. 2013), however it has a significantly shallower slope² of roughly $M^{-0.3}$. The distribution is established fairly quickly and is maintained until the collapse of the parent cloud ends. This mass function of bound structures is consistent with the cloud in cloud picture shown in Fig. 1 in that there is a vast hierarchy of bound structures embedded in each other.

Observationally finding the substructure of a GMC is very challenging, most observers instead concentrate on the so called *cores* which are collapsing clouds that have no self gravitating fragments. Figure 5 shows the total CMF (time and mass averaged over an ensemble of GMCs following the distribution shown in Fig. 3) for different initial parameters.

² In this paper the approximate high mass end behavior is estimated by fitting a power law between $0.5 M_{\odot}$ - $100 M_{\odot}$. The error presented in the figures only account for the uncertainty in the fitting.

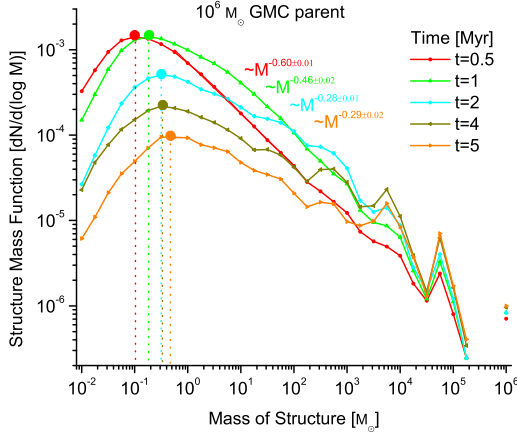


Figure 4. Time evolution of number of bound structures of different masses in a parent GMC of $10^6 M_{\odot}$. Here we count *all* self-gravitating structures, including clouds embedded in other clouds, cores etc. The plot is normalized so that integrated mass ($\int M \frac{dN}{d \log M} d \log M$) corresponds to the mass of gas bound in self-gravitating clouds relative to the total mass of the parent GMC, which explains the decreasing trend with time as more and more gas ends up in either protostars or becomes unbound. The upper end cuts off close to the parent GMC mass. The high mass power law fitting is done according to Footnote 2.

The simulated CMF reproduces the shape of observed results, having both a turnover point and a slightly shallower high mass slope ($\sim M^{-1.15}$) than the canonical Salpeter result of $\sim M^{-1.35}$ for the IMF (see [Offner et al. 2013](#)).

Fig. 6 clearly shows that there is very small difference between the CMF turnover masses and high mass slopes between GMCs of different sizes after 1 Myr. This is because early collapse is roughly isothermal so these clouds all have the same characteristic fragment mass (M_{crit} , see Eq. 19 for details). During later evolution the GMCs heat up at a different pace as the dynamical times are different. Meanwhile Fig. 7 shows that there is a clear trend of increasing turnover mass with time in each cloud. This phenomenon and its possible cause is further investigated in Sec. 3.2.

3.2 Evolution of the PSMF

We now examine the mass function of the final collapsed objects, the protostellar system mass function (PSMF).

In Fig. 8 we show that parent clouds of all masses produce similar to Salpeter scalings the high mass end with lower mass clouds producing slightly steeper slopes. Also, there is a clear trend of increasing turnover mass with increasing parent mass, unlike the case of the CMF (See Fig. 6). It is worth noting that the GMC mass function is top heavy, which means that the high mass clouds dominate the integrated mass function. If we accept this result then it suggests a possible observational bias of the IMF as most observations focus on smaller clouds in the Milky Way. Also, turbulent fragmentation does not produce a cloud mass dependent “maximum stellar mass”.

The increasing turnover mass for both PSMF and CMF is related to the equation of state. In a turbulent cloud, self

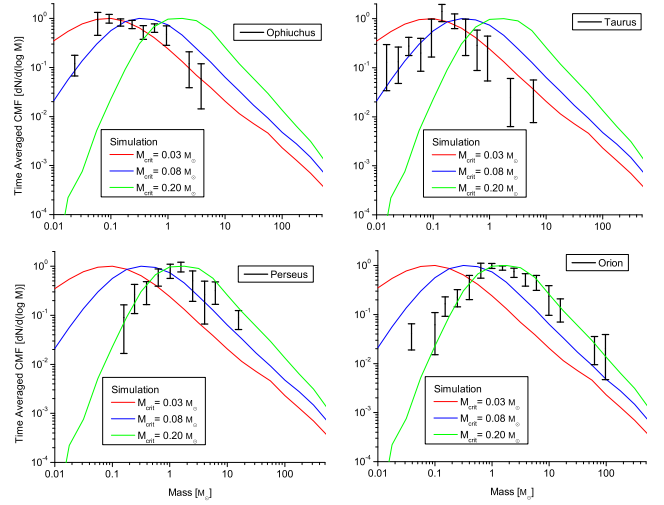


Figure 5. Comparison of the average simulated CMF with the observed CMF by [Sadavoy et al. \(2010\)](#) in different clouds in the Milky Way (the plot is normalized so that the peak of the CMF is set to unity). Note that observations which are below the completeness limit are also included (see the original paper for details). The simulated CMFs are averaged both over time (assuming the age of GMCs is uniformly distributed in the [0,5] Myr range) and the GMC mass function (following Fig. 3). The different initial critical masses in this case reflect having different T/Q_{coll} values, for definition see Eq. 19.

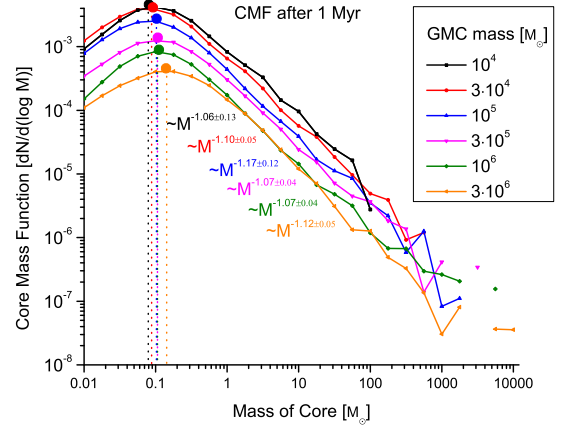


Figure 6. The CMF in GMCs of different masses 1 Myr after collapse starts for each cloud. The plot is normalized so that integrated mass corresponds to the relative mass of gas bound in cores, the peaks are denoted with solid circles. The high mass power law fitting is done according to Footnote 2. Both the turnover mass and the high mass slope exhibit very little sensitivity to the mass of the parent GMC.

gravitating fragments of different sizes form, which (according to the EOS of Eq. 6) have different effective polytropic indices. According to the EOS there exists a threshold in the surface density (Σ_{crit}) above which $\gamma > 4/3$, stabilizing the cloud against further fragmentation. Thus it is instructive to find the critical mass (M_{crit}) corresponding to Σ_{crit} . Using

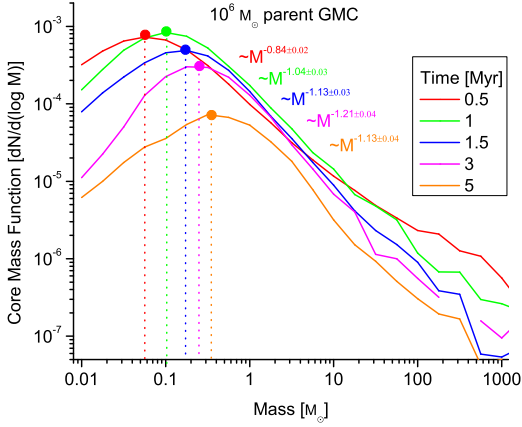


Figure 7. Time evolution of the CMF in a parent GMC of $10^6 M_{\odot}$. The plot is normalized so that integrated mass corresponds to the mass of gas bound in self gravitating clouds relative to the total mass of the parent GMC, which explains the downwards trend since less and less gas is bound in cores as more protostars are produced and the cloud gets heated by contraction. The high mass power law fitting is done according to Footnote 2. There is a clear trend in the turnover mass (the peaks are denoted with solid circles) which increases significantly while preserving the overall shape of the function (e.g. high mass slope).

the collapse condition of Eq. 7 and expanding up to linear order in γ around 1 (this is a good approximation during most of the cloud’s lifetime as the collapse starts at close to isothermal conditions) yields that $\Sigma > \Sigma_{\text{crit}}$ requires that

$$R < R_{\text{crit}} = R_0 \frac{\gamma \left(\frac{\Sigma_{\text{crit}}}{\Sigma_0} \right)^{\gamma-1}}{\frac{\Sigma_{\text{crit}}}{\Sigma_0} \left(1 + \mathcal{M}_{\text{edge}}^2 \right) - \mathcal{M}_{\text{edge}}^2 + \gamma - 1}, \quad (17)$$

where R is the fragment radius and R_0 , Σ_0 , $\gamma = \gamma(\Sigma_0)$ are the radius, surface density and the effective polytropic index of the parent cloud. From Eq. 17 we can find the critical mass $M_{\text{crit}} = 4\pi R^2 \Sigma_{\text{crit}}$ below which fragments are unlikely to collapse (note: according to the EOS of Eq. 6 the critical surface density $\Sigma_{\text{crit}} \approx 2400 M_{\odot}/\text{pc}^2$). These formulas can be simplified by assuming isothermal collapse ($\gamma \simeq 1$) and that the parent GMC is highly supersonic ($\mathcal{M}_{\text{edge}}^2 \gg 1$), Eq. 10 yields then:

$$R_{\text{crit}} \approx \frac{R_0 \Sigma_0}{\mathcal{M}_{\text{edge}}^2 \Sigma_{\text{crit}}} = R_{\text{sonic}} \frac{\Sigma_0}{\Sigma_{\text{crit}}}. \quad (18)$$

Using the mass-size relation of Eq. 9 and that $R_0 \gg R_{\text{sonic}}$ we obtain

$$M_{\text{crit}} \approx \frac{4\pi R_{\text{sonic}}^2 \Sigma_0^2}{\Sigma_{\text{crit}}} = \frac{M_{\text{sonic}}^2}{16\pi R_{\text{sonic}}^2 \Sigma_{\text{crit}}} = \frac{c_s^4}{4\pi G^2 Q_{\text{coll}}^2 \Sigma_{\text{crit}}} \propto \frac{T^2}{\Sigma_{\text{crit}}}. \quad (19)$$

The critical mass only depends on the cloud temperature and the equation of state.

Fig.9 shows the time evolution of the time and ensemble averaged PSMF for different initial M_{crit} values (the different critical masses in these cases arise from having different $\sigma/Q_{\text{coll}}\Sigma_{\text{crit}}$; where we fix Q_{coll} and Σ_{crit} and vary T_{init} , for definition see Eq. 19) which all produce a shape similar

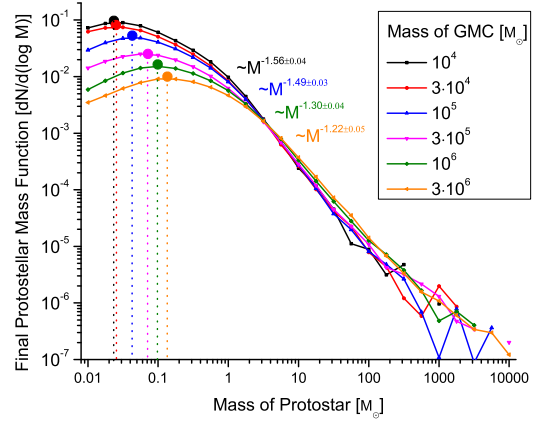


Figure 8. Protostellar system mass function (PSMF) after collapse ends (with no feedback) in parents of different masses assuming our simple equation of state. The Salpeter slope is always present (the high mass power law fitting is done according to Footnote 2). For these assumptions there appears to be “too many” brown dwarfs, and too much dependence on the parent GMC mass. These are the direct consequences of the EOS of the gas.

to the IMF but with different peak masses. If we compare the results to the canonical IMF fitting functions of Kroupa (2002) and Chabrier (2005), then it is clear that the average PSMF always reproduces the Salpeter scalings however the turnover point is heavily influenced by $T/Q_{\text{coll}}\Sigma_{\text{crit}}$. Since Q_{coll} is a constant this implies that the average temperature of the cloud could have a significant effect on the turnover point if Σ_{crit} is constant.

Fig. 10 shows how this critical mass evolves in time for our default model assumptions ($\Sigma_{\text{crit}} = \text{const.}$). It is clear that M_{crit} correlates well with the peaks of the PSMF of the corresponding time interval.

This increase of the critical mass with time has an interesting consequence. Fig. 11 shows that the average time of formation monotonically increases with the protostellar system mass.

So, if the equation of state does not depend on temperature (e.g. our $\gamma(\Sigma)$ is invariant) then the turnover mass shows a strong ($\propto T^2$) dependence on the initial conditions which would likely lead to a non-universal IMF. A possible solution to this issue is if Σ_{crit} has a temperature dependence. An example is provided by Krumholz (2011), where the initially formed protostar ‘seed’ heats up its environment, preventing it from collapsing. It can be shown that in leading order this leads to roughly $\Sigma_{\text{crit}} \propto T^2$ which would produce a constant M_{crit} , and thus a universal IMF.

Fig. 12 compares the results of two simulations, one with $\Sigma_{\text{crit}} = \text{const.}$ and one with $\Sigma_{\text{crit}} \propto T^2$. Although the latter still shows some time dependence, the shifting of the peak is greatly reduced, making it more consistent with observations, even though the only assumption about feedback was that it prevents collapsed cores from accreting from their surroundings.

An important question of star formation is what fraction of the gas ends up in stars. The analytical excursion set

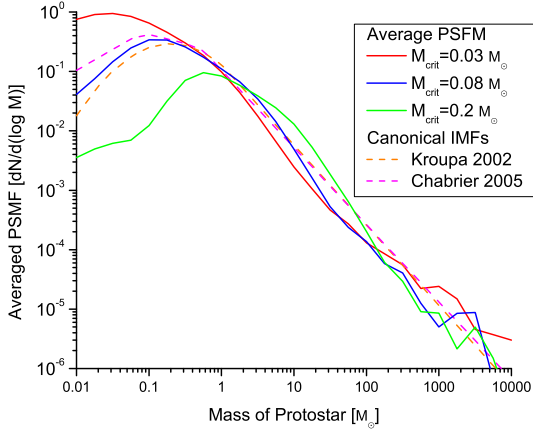


Figure 9. Evolution of the averaged PSFM (normalized to integrated mass) for different initial critical masses (set by having different $T/Q_{\text{coll}}\Sigma_{\text{crit}}$ values, for definition see Eq. 19) compared to the canonical IMF of Kroupa (2002) and Chabrier (2005). The PSFM is averaged both over time (assuming the age of GMCs is uniformly distributed in the [0,5] Myr range) and the GMC mass function (following Fig. 3). We included the standard $M_{\text{crit}} = 0.03 M_{\odot}$ (solid red), an $M_{\text{crit}} = 0.08 M_{\odot}$ (solid blue) and an $M_{\text{crit}} = 0.2 M_{\odot}$ (solid black) scenarios. Although the shape is similar, there is a clear shift of the peak to higher masses with increasing M_{crit} . At the high mass end turbulent fragmentation produces an average slope close to the Salpeter result in all cases.

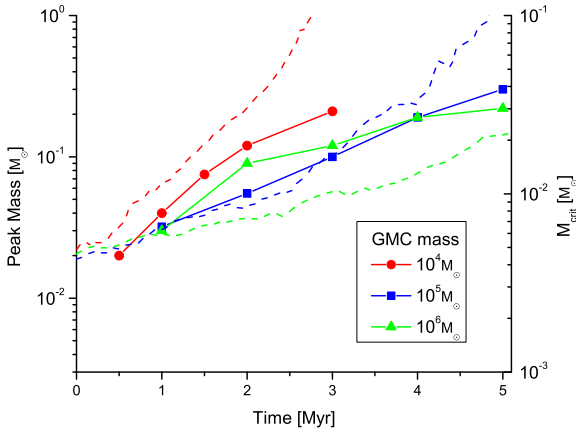


Figure 10. The peak masses of the PSFM of different time intervals (solid line with symbols) and the critical mass (dashed lines) for different parent GMC masses according to Eq. 17. The critical mass correctly predicts the qualitative evolution of the peak mass.

models like in Paper I could not answer that question. With this model for GMCs of all sizes we get a star formation efficiency of roughly 5%-8% regardless of using a $\propto T^2$ or a constant Σ_{crit} .

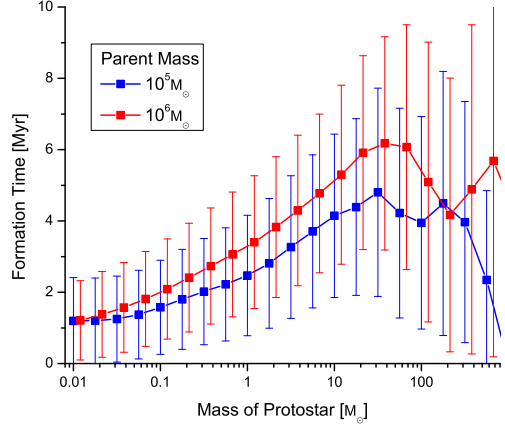


Figure 11. Average time of formation for protostars of different masses (the error bars represent the standard deviation) in a model with an *invariant* EOS. There is a clear trend of more massive protostars forming at later times (which is consistent with the shifting of the turnover mass in Fig. 10), however the scatter is comparable to this difference. Nevertheless it is clear that most massive stars only start forming after roughly a Myr after the cloud starts collapsing.

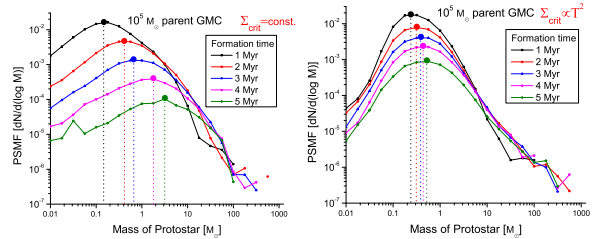


Figure 12. PSFM for protostars in a parent GMC of $10^5 M_{\odot}$ for an EOS with $\Sigma_{\text{crit}} = \text{const.}$ (left) and for an EOS with $\Sigma_{\text{crit}} \propto T^2$ (right). The solid circles show the peaks, which move considerably less for the $\Sigma_{\text{crit}} \propto T^2$ case. As implied by Eq. 19, if $\Sigma_{\text{crit}} \propto T^2$ then $M_{\text{crit}} \sim \text{const.}$, and the IMF becomes invariant.

4 CONCLUSIONS

The aim of this paper is to provide a general framework for the modeling of star formation through turbulent fragmentation from the scale of GMCs to the scale of stars. We propose a semi analytical extension of the model of Guszejnov & Hopkins (2015) (Paper I) that we believe is detailed enough to capture the physics essential for modeling the formation of stars without being too demanding numerically. Just like the analytical excursion set models it does not simulate turbulence directly, instead it assumes that the density follows a locally random field distribution. The density field however is directly resolved on a grid which preserves spatial and time information allowing the implementation of more detailed physics (e.g. proper checking for self gravitation, time dependent cloud collapse) and the analysis of the spatial structure. This is not possible in the excursion set formalism which describes the density field around a random

Lagrangian point. This also means that unlike the analytical models not 100% of the mass ends up in protostars.

The presented form of the model contains only the minimally required physics (turbulence, self gravity, some equation of state). It is however possible to integrate more sophisticated models to provide a more accurate description of these processes. Also, since the output of our model contain the time dependent evolution of the CMF and the PSMF, one can easily apply corrections during post processing to account for effects like protostellar fragmentation or supernova feedback (stop the evolution when enough SNe exploded).

By applying this framework to modeling the collapse of giant molecular clouds, we found that even the basic model qualitatively reproduces the observed core mass function. The CMF evolution has little dependence on the mass of the parent GMC mass.

Another result of the simulation is the mass distribution of all bound structures in the cloud. This appears to have the same shape as the CMF with a shallower slope of roughly $M^{-0.3}$ at the massive end. These clearly show the hierarchy of bound structures.

One of the main results of our basic model is the protostellar system mass function (PSMF) which is obtained by following the collapse of an ensemble of GMCs following a GMC mass function determined by Hopkins (2012b). As in Paper I we found that the PSMF is qualitatively very similar to the observed IMF: it exhibits a close to Salpeter slope almost independent of the initial conditions, while the turnover mass is mainly set by the equation of state and the initial temperature.

Due to the minimalistic nature of the model we managed to pinpoint the physical quantities influencing the different features of the PSMF and thus the IMF. We found that the Salpeter slope at the high mass end is a clear consequence of turbulence (as shown before in Paper I) where the inclusion of extra physics only causes slight deviation from the pure power law behavior. We also found that the mass function becomes shallower as we approach the sonic mass as the turbulence becomes subsonic below these scales. Furthermore we found that the actual turnover point is remarkably only set by the local temperature and the equation of state in leading order ($M_{\text{crit}} \propto T^2 / \Sigma_{\text{crit}}$).

We found that if we assume a $\gamma(\Sigma)$ equation of state then the PSMF for protostars of the same age changes as the parent cloud collapses: the turnover mass increases with time. This can be explained by the increase M_{crit} . This leads to a quadratic dependence of the turnover mass on the initial temperature which is inconsistent with the observed universality of the IMF. This means that it is not possible to derive a universal IMF with an equation of state that has no temperature dependence. One way to 'fix' the model is by implementing the feedback from protostars. Using the assumptions of Krumholz (2011) in leading order the heating from the protostars cancel the aforementioned quadratic scaling (due to $\Sigma_{\text{crit}} \propto T^2$), leading to a close to universal turnover mass.

ACKNOWLEDGMENTS

We thank Ralf Klessen and Mark Krumholz for their insights and inspirational conversations throughout the de-

velopment of this work.

Support for PFH was provided by the Gordon and Betty Moore Foundation through Grant #776 to the Caltech Moore Center for Theoretical Cosmology and Physics, an Alfred P. Sloan Research Fellowship, NASA ATP Grant NNX14AH35G, and NSF Collaborative Research Grant #1411920. Numerical calculations were run on the Caltech compute cluster "Zwicky" (NSF MRI award #PHY-0960291) and allocation TG-AST130039 granted by the Extreme Science and Engineering Discovery Environment (XSEDE) supported by the NSF.

REFERENCES

- Bolatto A. D., Leroy A. K., Rosolowsky E., Walter F., Blitz L., 2008, *ApJ*, **686**, 948
- Chabrier G., 2005, in Corbelli E., Palla F., Zinnecker H., eds, *Astrophysics and Space Science Library* Vol. 327, *The Initial Mass Function 50 Years Later*. p. 41
- Federrath C., Klessen R. S., Schmidt W., 2008, *ApJ*, **688**, L79
- Guszejnov D., Hopkins P. F., 2015, *MNRAS*, **450**, 4137
- Hennebelle P., Chabrier G., 2008, *ApJ*, **684**, 395
- Hopkins P. F., 2012a, *MNRAS*, **423**, 2016
- Hopkins P. F., 2012b, *MNRAS*, **423**, 2037
- Hopkins P. F., 2013a, *MNRAS*, **430**, 1653
- Hopkins P. F., 2013b, *MNRAS*, **430**, 1880
- Kroupa P., 2002, *Science*, **295**, 82
- Krumholz M. R., 2011, *ApJ*, **743**, 110
- Lada C. J., Lada E. A., 2003, *ARA&A*, **41**, 57
- Larson R. B., 1981, *MNRAS*, **194**, 809
- McKee C. F., Ostriker E. C., 2007, *ARA&A*, **45**, 565
- Murray J. D., 1973, *Journal of Fluid Mechanics*, **59**, 263
- Offner S. S. R., Clark P. C., Hennebelle P., Bastian N., Bate M. R., Hopkins P. F., Moraux E., Whitworth A. P., 2013, preprint, ([arXiv:1312.5326](https://arxiv.org/abs/1312.5326))
- Padoan P., Nordlund Å., 2002, *ApJ*, **576**, 870
- Padoan P., Nordlund A., Jones B. J. T., 1997, *MNRAS*, **288**, 145
- Press W. H., Schechter P., 1974, *ApJ*, **187**, 425
- Rosolowsky E., 2005, *PASP*, **117**, 1403
- Sadavoy S. I., et al., 2010, *ApJ*, **710**, 1247
- Schmidt W., Federrath C., Hupp M., Kern S., Niemeyer J. C., 2009, *A&A*, **494**, 127